`Vol. 6, No. 1, pp. 17-31, (March 2025)
DOI: 10.21608/aujes.2025.333541.1300
Aswan University Journal of Environmental Studies (AUJES)
Online ISSN: 2735-4237, Print ISSN: 2735-4229
Journal homepage: https://aujes.journals.ekb.eg/ E-mail: AUJES@aswu.edu.eg
Original research

Palm leaves -derived porous carbon materials for the elimination of Fe (II) ions from aqueous systems

Ahmed F. M. Ali,[1] Abdelaal S. A. Ahmed[1]*, Ahmed A. Gahlan[1]*, Abdel-Aziz Y. El-Sayed[1]

Chemistry department, Faculty of Science, Al-Azhar University, Assiut 71524, Egypt.

Received: 3 /11 /2024 Accepted: 1 / 3 /2025

Abstract:

Ferrous ion contamination in water is considered a complex and critical environmental problem due to rapid industrialization, human activity, and agricultural activities. Here, three adsorbent materials derived from palm leaves (PL), known as PL, modified PL (mPL) and biochar-derived PL (BPL) were prepared and utilized to eliminate Fe (II) from aqueous solution. The effects of pH, shaking time, amount adsorbent, and initial Fe (II) concentration were performed in a batch adsorption technique. The maximum removal of Fe (II) at initial concentration of 5 ppm, pH 5, contact time 80 min, and 0.05 g were 77. 96, and 86% for the PL, mPL and BPL, respectively. The kinetic study showed that the adsorption of Fe (II) ions onto our adsorbents obeyed the pseudo-second-order kinetic model. Furthermore, the adsorption isotherms confirm that the adsorption of Fe (II) ions onto the PL, mPL and BPL obeyed the Langmuir model, verifying the chemical adsorption mechanism. Palm leaves proved high adsorption efficiency toward Fe (II) ions in the aqueous media.

Keywords: palm leaves, ferrous ions, adsorption, biochar, agricultural waste physio-chemical modification.

1- Introduction

No one can deny that there is no life without water, typically water constitutes about 75% of our bodies (Popkin et al., 2010 ; Dutta et al., 2021). The increasing population in the world is an important factor that should be considered to wisely use each drop of water, keep our freshwater away from pollutants, as well as treat the polluted water resources. The increase in industrialization plays a big role in water pollution, and thus a great effort has been devoted to overcoming these problems. In contrast to other pollutants in the environment, such as household and petroleum hydrocarbons, trace metals can accumulate to hazardous levels covertly. Typically, heavy metals are used to describe these metals with a higher density than water which can cause toxicity at low levels of exposure (Abdelmonem et al., 2024; Cheira et al., 2024; Türkmen et al., 2022). Recently, the poisoning of heavy metals became a serious environmental issue (Mungondori et al., 2017).

Corresponding author*: E-mail address: hamedharoun42@azhar.edu.eg; abdelaalsaiyd@azhar.edu.eg

The big problem with heavy metals is that they are nondegradable over time, and thus they are considered continuous hazard sources. Stricter laws have been enacted in many nations to reduce water pollution. The maximum allowed limits for the release of hazardous heavy metals into aquatic systems have been established by several regulatory agencies. Typically, iron is a corrosive metal and is a main substance in the effluents of many industries (Dey et al., 2022). Iron ion is needed in plant metabolism and is considered a vital metal for humans, but its presence in water at a concentration higher than the standard level (0.3 mg/L) is considered toxic, leading to many health problems like diabetes, poor growth, and heart failure (Moghadam et al., 2013). The permissible limit for industrial effluent discharge set by the World Health Organization (WHO) for iron is in the range of 0.1-1 mg/L. Ion exchange, chemical precipitation, photocatalysts, electrochemical deposition, and flotation are famous techniques used for the remediation of various pollutants from wastewater.(Abdelmonem et al., 2024; El-Sawaf et al., 2024; Li et al., 2023; Tolan et al., 2024) The high cost, using toxic chemicals, and consuming time are the main factors restricting their large-scale applications (Kamalesh et al., 2023). Adsorption techniques have acquired much concern over the years. Typically, adsorption is used to uptake various contaminants from their solutions with low cost as well as with relatively high removal performance. (Mungondori et al., 2017) Recently, great attempts have been made to remediation of heavy metals by low-cost affordable agricultural wastes via adsorption techniques such as plants leaf, (Dey et al., 2022; Ezeonuegbu et al., 2021) sawdust, (Meez et al., 2021) rice husk (Yefremova et al., 2023) …etc. Palm leaves (PL) are an agricultural waste substance, structurally consisting of cellulose, hemicellulose, and lignin. Palm trees are superabundant in many countries in the world, the total weight of date palm waste produced in the world is 4.5 million tons. The presence of various functional groups such as OH^-, COO^-, …etc., make PL expected to be good heavy metal bio-sorbents (Abu Al-ub, 2006). The application of agriculture wastes displayed an important role for high chemical oxygen demand (COD) and biological oxygen demand (BOD) issues due to the high released soluble organic compounds. So, treatment of the adsorbents surfaces using oxidizing agents, base solutions, or mineral acids are very important. These agents are used to activate the surface increasing its chelating sites and porosity which is effective for heavy metal removal from wastewater (Sarker et al., 2017). Biochar has attracted remarkable attention as an adsorbent for remediation of various pollutants.(Reda et al., 2022) Biochar is a carbon form that is characterized by fine structure, high surface area, and porosity with multiple functional groups that promote the adsorption of targeted pollutants. Pyrolysis of wood, manure, grass, sludge, and food waste are the main ways for producing biochar. Agricultural waste materials such as palm leaves are preferred as feedstock for biochar preparation due to their eco-friendliness and abundance with low cost (Khalid M. Khader, 2022; Krajčovičová et al., 2023). In this study, unmodified-PL, modified palm leaves (mPL) and biochar palm leaves (BPL) were utilized for the remediation of Fe (II) ions from wastewater by adsorption process. Chemical treatment and pyrolysis enhance the surface area of the adsorbent material, and this enhances the removal of metal ions. The effect of pH, shaking time, the amount of adsorbent, and initial Fe (II) ion concentration on overall removal efficiency were investigated. In addition, the adsorption isotherms and kinetics were studied to confirm the adsorption process.

2 Materials and methods

2.1 Chemicals

Sodium hydroxide (NaOH, ≥ 98%, pellets anhydrous), hydrochloric acid (HCl, 37%), hydroxylamine hydrochloride ($NH_2OH.HCl$ 99%), potassium permanganate ($KMnO_4$ ≥ 99%), ammonium acetate ($NH_4C_2H_3O_2$ 98-100.5%), glacial acetic acid (CH_3COOH > 98 %), 1,10-phenanthroline monohydrate ($C_{12}H_8N_2.H_2O$ ≥ 98%), Sulphuric acid (H_2SO_4 95-97%), and ferrous ammonium sulfate ($Fe(NH_4)_2(SO_4)_2.6H_2O$ ≥ 99%) purchased from Merck, Darmstadt, Germany. All utilized chemicals studied were of analytical grade. All preparations in our study were performed with distilled water obtained from an ultrapure purifier (Ultra-pure, resistivity ≥ 18.2 MΩ).

2.2 Preparation of adsorbent derived from PL.

The PL samples were collected from agricultural lands located at Awlad Salem Bahri village, Dar-Eslam city, Sohag, Egypt. The collected PL washed thoroughly with tap water, then washed twice with distilled water and allowed to dry. Then, the dried PL sample was ground into fine powder and sieved for particle size 63 µm. The dried powder was washed with distilled water and separated by decantation and filtration. Finally, the obtained PL was subjected to drying at 105 ^oC for 2 h. Followed by grinding well with a mortar and then being packed in a bottle, and the obtained powder known as PL.

For the chemical-modified PL (mPL), a certain weight of dried PL was suspended for 30 min in a mixture of NaOH (0.01 M) with trace of $KMnO_4$ until the solution became slightly pink with a ratio of 0.005 g adsorbent/0.25 mL mixture. After that, the biomass was washed thoroughly with dist. water until pH ≈ 7. The filtration was discharged, and the mPL was dried in an oven at 105 ^oC for 2 h, ground well with a mortar and then packed in a clean plastic bottle, the obtained powder known as mPL. In the case of biochar-derived PL, a certain amount of PL is put in a ceramic crucible. The vessel was placed in a gradient temperature furnace at 300 ^oC. The mass of material after the pyrolysis process was grounded well with a mortar and packed in clean plastic bottles; the obtained black material is known as BPL.

2.3 Characterization and measurements

Spectrophotometer (model: CECIL3021, Cambridge, England), pH meter (Adwa model AD110, Romania), drying oven (bender, Germany), shaking standard testing sieves (model: FTL0200 "IRIS", Filtra, Spain), muffle furnace (model: LH 60/12, Nabertherm GmbH, Germany), a sartorius balance and grinding equipment were used for sample preparation. Fourier transfer infra-red (FTIR) was used to define the functional groups existing in the adsorbents. Scanning electron microscopy (SEM) (model: JEOL JSM-5500 LV, Japan) to investigate the morphology of the adsorbent materials. The N_2 adsorption-desorption technique was applied (model: BEL SORP MAX, Japan) to measure total pore volume, specific surface area, and mean pore diameter of the prepared adsorbent materials.

2.4 Adsorption ferrous ions

A batch adsorption procedure was used to remove ferrous ions. Several factors affected the adsorption process, including shaking time, pH, the amount of used adsorbent, and the initial Fe (II) ion concentration at room temperature (25±1 ^0C), particle size was adjusted at 63 µm, volume of solution 50 mL and shaking speed of 130 rpm. The initial pH of the solutions was adjusted by 0.01M HCl and NaOH. After establishing adsorption equilibrium, the filtrate was analyzed by the phenanthroline method using a spectrophotometer to determine the concentration of the Fe (II)

ions. (Tamura et al., 1974) The experiments were performed in triplicate to validate the results obtained. Removal percentage (R%) of Fe (II) ions was calculated by **Eq. 1**. The adsorption capacity at equilibrium (q_e; mg/g) was calculated by **Eq. 2**.

$$R\ (\%) = \frac{C_0 - C_e}{C_0}\ X\ 100 \qquad (Eq.\ 1)$$

$$q_e = \frac{(C_0 - C_e)}{M}\ V \qquad (Eq.\ 2)$$

Where C_0 and C_e are the initial and final Fe (II) concentrations (mg/L), respectively. V is the solution volume (L), and M is the mass of the absorbent (g).

3 Results and discussion

3.1 Physicochemical Characterizations

The surface area was estimated by Brunauer-Emmett-Teller (BET) at 77K (-196°C). As seen from **Table 1**, the modification breaks the lignin structure, improving the penetration of the modifying agent, which increases the number of oxygen-containing functional groups and thus increases the surface area and pore volume. Additionally, the surface area and pore volume for BPL became larger due to thermal action at 300 °C. However, some oxygen-containing functional groups undergo thermally decomposed and react with carbon materials to generate small molecular gases such as CO, CO_2 and water vapor during the high-temperature activation process. In the meantime, the morphology and structure of carbon materials will also change to a certain extent, thereby increasing the specific surface area of carbon materials.(Qiu et al., 2023)

Table 1: The specific surface area and pore diameter of the PL, mPL, and BPL adsorbent materials.

Biosorbent	BET surface area (m^2/g)	Pore volume (cm^3/g)	Mean pore diameter (nm)
PL	1.71	3.91	9.15
mPL	3.74	4.92	5.25
BPL	6.51	6.35	3.90

As in FT-IR spectra (**Figure 1)**, the PL displayed the presence of O–H, N–H, C–H, C=O, C=C, C–N, C–O and C–H groups. This provides excellent adsorptive property with pollutant interaction. The broad band of O–H and N–H groups at 3420 cm^{-1}. The presence of peaks at 2920 and 2852 cm^{-1} was assigned for the stretching of CH, CH_2 and CH_3 groups. The bands centered in 1736 cm^{-1} are for the C=O groups. The C=C group of the aromatic ring of lignin was at 1513 cm^{-1}. Also, the aromatic CH_3 group at 1460 cm^{-1} was compatible with the presence of the aliphatic part of lignin. The peak at 1430 cm^{-1} was assigned for the CH_2 bending. The peaks between 1323 and 1059 cm^{-1} are assigned for C−O for the COO^- groups. Modification leads to shifts in some groups, while the pyrolysis leads to shifts and disappearance of some groups, as well as the appearance of a peak at 1590 cm^{-1} which could be attributed to dehydration, dehydrogenation, and deoxygenation reactions at elevated temperatures. Furthermore, the FTIR spectra of mPL after Fe (II) adsorption displayed some changes as observed for disappearing the small beak located at 460 cm^{-1}, which indicates a chemical adsorption as confirmed by adsorption kinetic and isotherm analysis in the following sections.

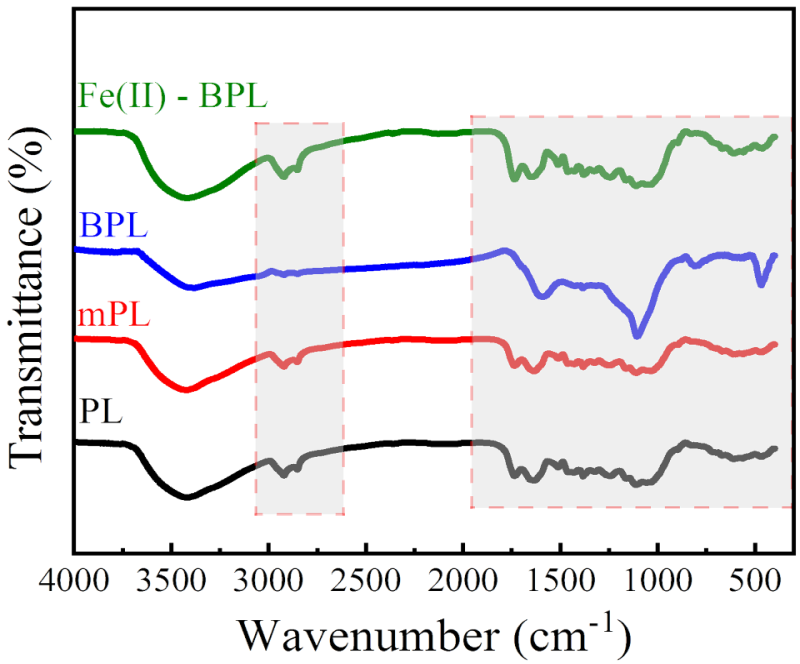

Figure 1: FT-IR spectra of PL, mPL, and BPL adsorbents and mPL after Fe(II) adsorption.

The morphology of the prepared adsorbent materials was examined by SEM. From **Figure 2,** the morphology of the PL and mPL samples is clearly different, and the surface of mPL is porous. The morphology of mPL samples before and after adsorption displayed a different morphology. The surface is transformed to be more compact, smoother, and with fewer open pores due to the binding of Fe (II) ions on the surface of mPL, which is in agreement with previous literature.(Ali et al., 2024) The SEM image of BPL in **Figure 2c** revealed a rough and irregularly sized and shaped highly porous surface with multiple voids and micropores providing sufficient space for the adsorption process.

3.2 Adsorption study

As seen in **Figure 3a,** the removal of Fe (II) ions by the PL increased by increasing the pH, and the maximum removal percentage was achieved at pH ≈ 5. The degree of ionization on the adsorbent surface by increasing the pH illustrated the increase in removal. At low pH, the high H^+ concentrations compete with Fe (II) ions. Thus, the binding sites become protonated and thus decrease the adsorption of Fe (II) ions. At high pH values, the lower H^+ concentration enhanced the adsorption of Fe (II) ions. To prevent metal precipitation, which could interfere with or be mistaken for adsorption, pH greater than seven was not explored as the solubility constant (K_{SP}) of Fe $(OH)_2$ is $4.87x10^{-17}$. The reduction in metal uptake at an increased pH beyond its optimum value is attributed to reduced solubility and precipitation. Therefore, all steps of the adsorption processes were carried out with a pH ≈ 5 (Herbert et al., 2021). As shown in **Figure 3b,** by increasing the adsorbent dose, the removal of Fe (II) ions gradually increased due to increasing the number of active sites available for bonding with the adsorbate ions.(Abdelrazek et al., 2025) The optimum dose of absorbent was 0.05 g, and further increasing in the adsorbent doses displayed non-noticeable enhancement.

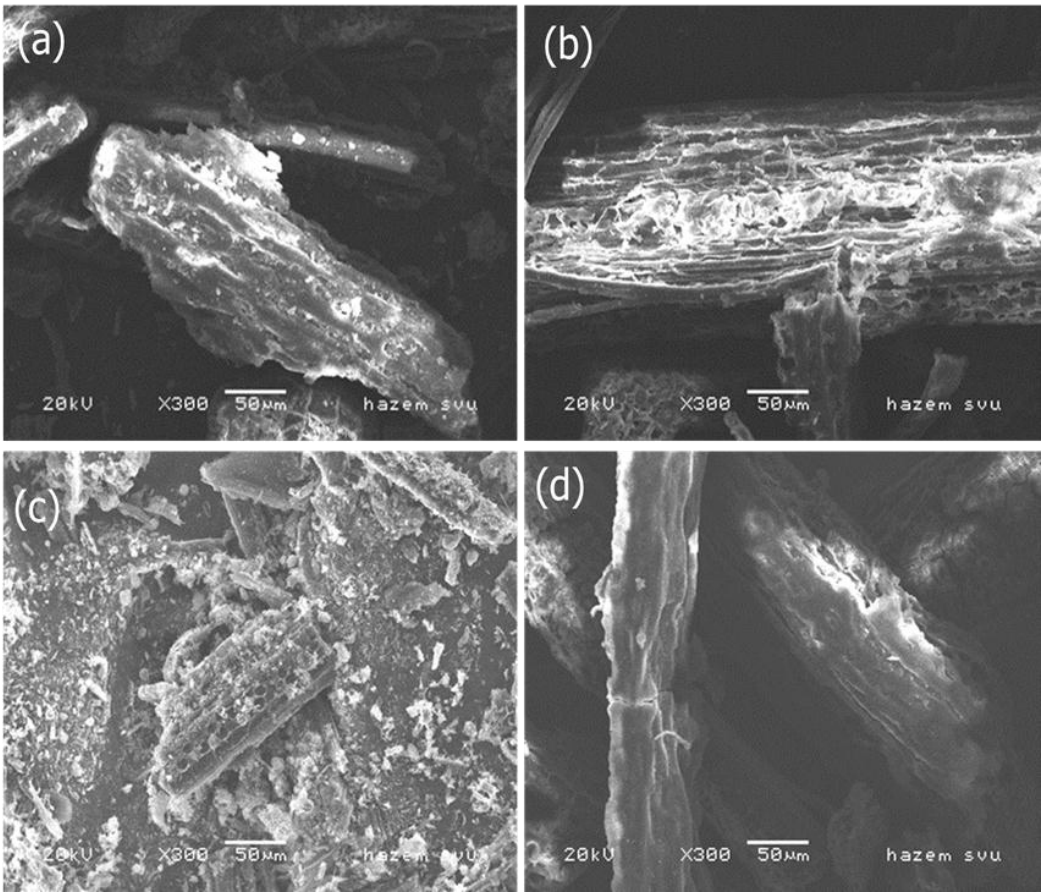

Figure 2: SEM of (a) PL, and (b) mPL before adsorption. SEM of (c) BPL, and (d) mPL after adsorption.

The effect of contact time on the removal of Fe (II) ions by PL in **Figure 3c** displayed a gradual enhancement in the removal efficiency by increasing the contact time, followed by slowing down till reaching the equilibrium state, and the optimum time is 80 min. This may be attributed to the reaction between the Fe (II) ions and the functional groups of the PL, which led to the adsorption sites being progressively occupied. This time is very small in comparison with the time consumed for adsorption of Fe(II) by biochar synthesized from arabica coffee husks. (Guimarães et al., 2020) and close to the time consume to achieved maximum adsorption of Fe (II) by carbon derived from agricultural waste.(Nilavazhagi & Felixkala, 2021)

Figure 4 shows the impact of the initial Fe (II) ions concentration on the overall removal percentage (R%). By increasing the initial Fe (II) ions concentration from 5 to 25 mg/L, the removal percentage of Fe (II) ions was reduced from 77 to 22% for PL, 96 to 37% for mPL, and 86 to 28% for BPL. One possible explanation for the decline in removal efficiency observed upon elevating the concentration of Fe (II) ions is the saturation of sorption sites within a specific mass of adsorbent material.(Maneechakr & Karnjanakom, 2017)

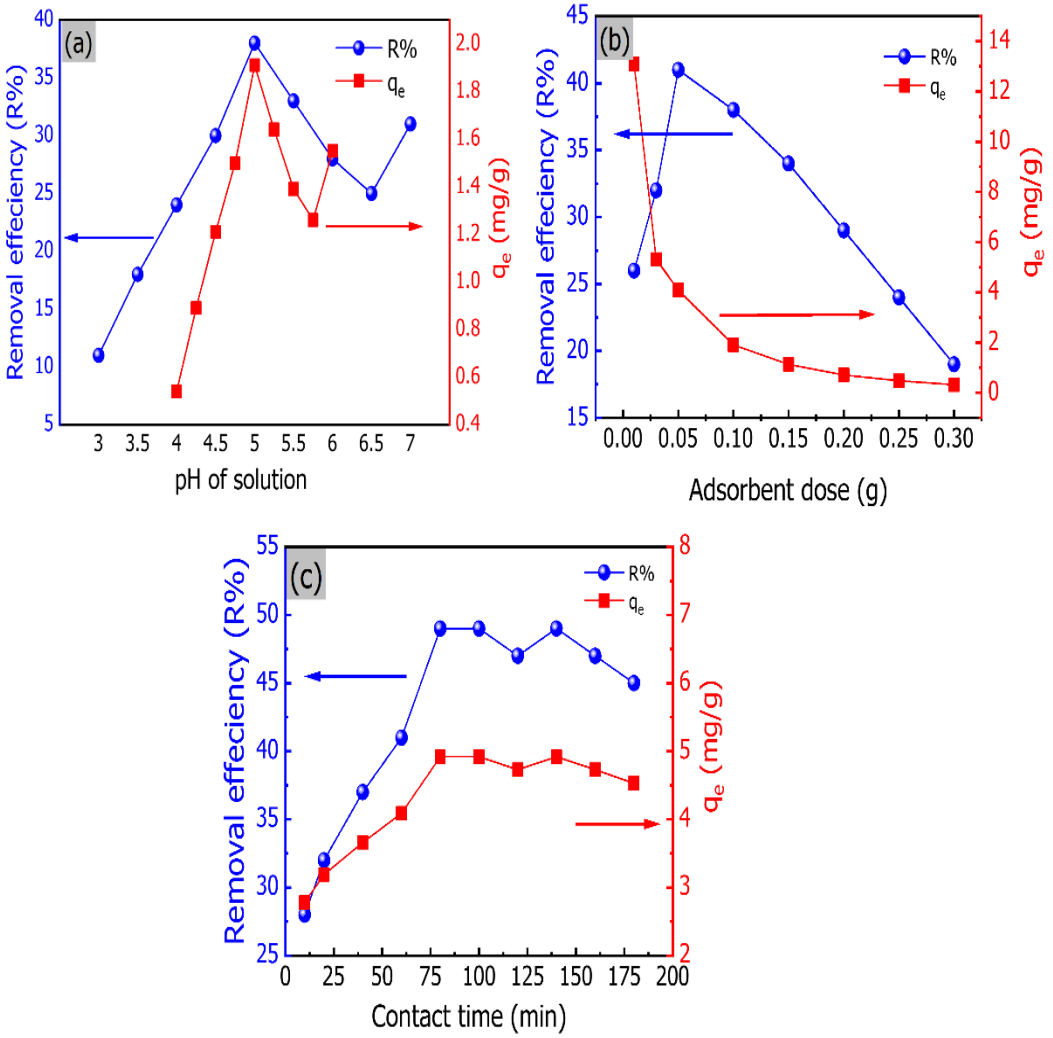

Figure 3: Effect of (a) pH, (b) adsorbent amount, and (c) shaking time on the removal of Fe (II) ions by PL. [V = 50 ml, adsorbent dose = 0.1g, t = 60 min, shaking speed is 130 rpm, C_0 =10 ppm].

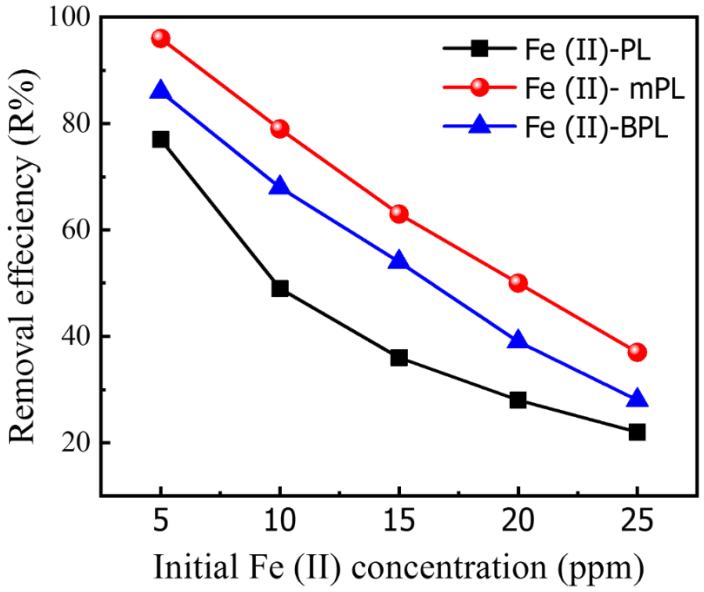

Figure 4: The relation between the initial Fe (II) concentration and the removal efficiency by PL, mPL, and BPL adsorbents [pH=5, t=80 min, dose = 0.05g].

3.3 Adsorption isotherms

Two adsorption isotherm models were applied to study the experimental data from the adsorption of Fe (II) ions. These models are Langmuir (Eq. 3) and Freundlich (Eq. 4) (Wang et al., 2019) (Ramos et al., 2014).

$$\frac{C_e}{q_e} = \frac{1}{(q_{max} * b)} + \frac{1}{q_{max} * C_e} \qquad \text{Eq. (3)}$$

$$Lnq_e = LnK_f + \left(\frac{1}{n_f}\right) lnC_e \qquad \text{Eq. (4)}$$

Where C_e is the equilibrium Fe (II) ions concentration (mg/L), q_e is the equilibrium adsorption capacity (mg/g), q_{max} is the maximum adsorption capacity, b is the Langmuir constant, K_f and n_f are the Freundlich constants.

The estimated parameters from adsorption isotherm models are listed in **Table 2**. Based on the correlation coefficient (R^2), the experimental data of the adsorption of Fe (II) ions on PL, mPL, and BPL were fitted well with the Langmuir model as in **Figure 5 (a, b).** This implies that a surface with uniform coverage of localized adsorption sites has produced a dye monolayer.(Askari et al., 2023) The interaction between an absorbent and an adsorbate is typically described by the Langmuir constant b. The b values form the adsorption of Fe(II) on the mPL are greater than those for adsorption by PL, and BPL adsorbents, as in **Table 2**. This suggests that the interactions with mPL and Fe (II) ions are the most stable ones.

Table 2: The parameters estimated from adsorption isotherm models.

Adsorbent	Langmuir			Freundlich		
	q_{max} mg/g	b L/mg	R^2	K_f (mg/g). (L/mg)$^{1/n}$	n_f	R^2
PL	5.621	1.953	0.997	3.874	7.628	0.923
mPL	9.671	4.457	0.996	6.503	5.734	0.926
BPL	8.019	1.332	0.999	4.785	5.970	0.974

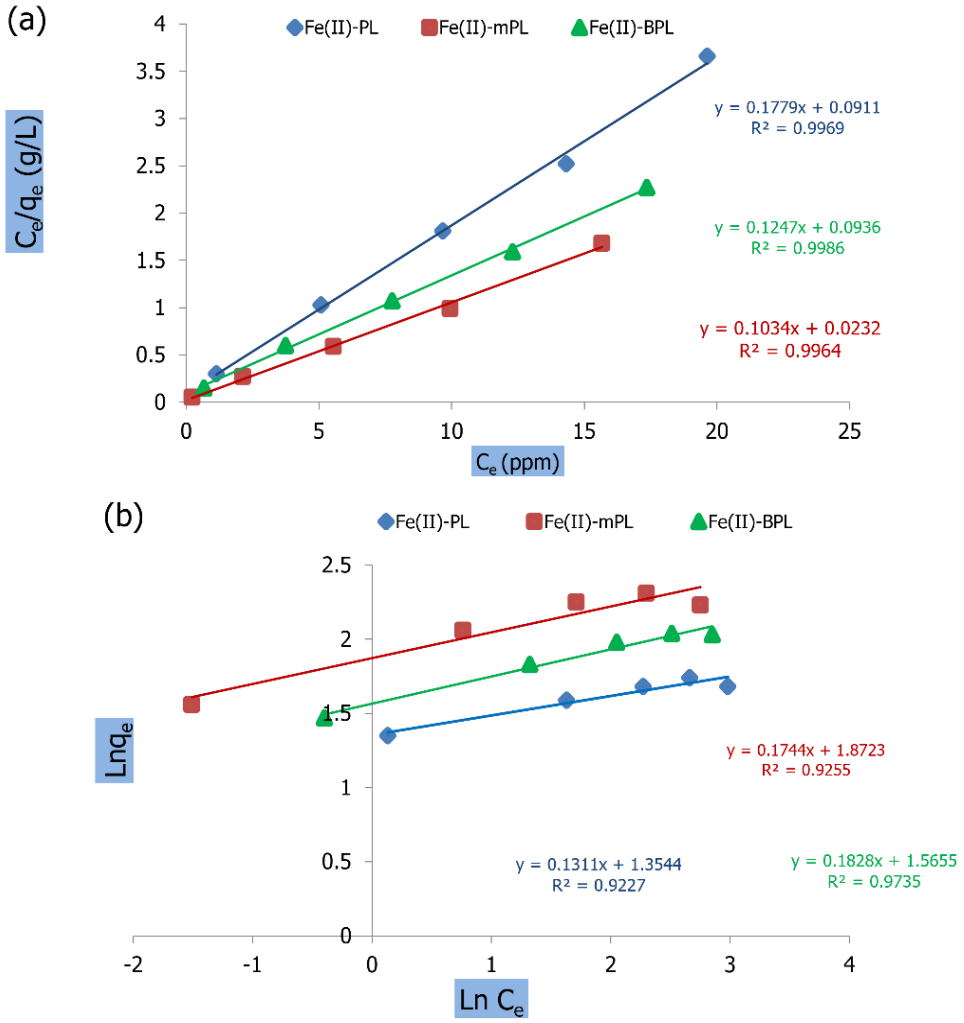

Figure 5: (a) Langmuir, and (b) Freundlich adsorption isotherm models.

3.4 Adsorption kinetics

Pseudo-first order, pseudo-second order, and intra-particle diffusion rate kinetic models were applied to study and describe the adsorption kinetics of ferrous ions as presented in **Eq. 5**, (Zhu et al., 2010) **Eq. 6 (Ali et al., 2024)**, and **Eq. 7** (Ramos et al., 2014), respectively.

$$\mathrm{Ln}(\mathrm{q_e} - q_t) = \mathrm{Lnq_e} - K_1 * \mathrm{t} \qquad \text{Eq. (5)}$$

$$\frac{t}{q_t} = \frac{1}{(k_2 * q_e{}^2)} + \frac{t}{q_e} \qquad \text{Eq. (6)}$$

$$q_t = k_p * t^{\frac{1}{2}} + C \qquad \text{Eq. (7)}$$

Where q_e (mg/g) is the equilibrium adsorption capacity, q_t (mg/g) is the adsorption capacity at time t. K_1 is the rate constant (l/min) of the pseudo-first order reaction, and K_2 is rate constant of the pseudo second-order reaction (g/mg.min), K_p is the rate constant of intra-particle diffusion ($mg/g.min^{1/2}$) and C (mg/g) is the intercept, which is identified with the thickness of the boundary layer.

The estimated parameters along with their correlation coefficients from **Figure 6(a-c)** are listed in **Table 3**. Higher R^2 values suggest that the pseudo-second-order kinetic model adequately fits the experimental data of Fe (II) adsorption on PL, mPL, and BPL adsorbents. By using PL, mPL, and BPL adsorbents, the estimated q_e for Fe (II) was 4.92, 7.190, and 6.11 mg/g, respectively. From Table 3, all values are better than those estimated from the pseudo-first order. This demonstrated that the adsorption is chemical process, which is lined with the FTIR data as well as the adsorption isotherm data as mentioned above. Usually, the adsorption mechanism can be controlled by various ways, the most limiting step is the diffusion mechanism such as intra-particle and external diffusion.(Ozcan et al., 2006) Consequently, to estimate the rate-controlling step of the adsorption process, the intra-particle diffusion model was investigated. It was found that the experimental data least fit the intra-particle diffusion model. Therefore, the entire adsorption process can be controlled by intra-particle diffusion and external mass transfer. From the discussion above, we can conclusion that the the experimental data for adsorption Fe (II) onto the adsorbent materials were fitted by the pseudo-second-order model. This suggests that the chemisorption process, which entails the exchange of electrons between the absorbent and adsorbate, is most likely the rate-limiting step. (Denizli et al., 2000)

Table 3: Estimated kinetic parameters for removal of Fe (II) by PL, mPL, and BPL adsorbents.

Kinetic model	Parameter	Adsorbents		
		PL	**mPL**	**BPL**
Pseudo-first order	$q_{e,cal}$ (mg/g)	1.927	2.900	2.431
	K_1 (min^{-1})	0.019	0.024	0.018
	R^2	0.644	0.815	0.911
Pseudo-second order	$q_{e,exp}$ (mg/g)	4.920	7.190	6.110
	$q_{e,cal}$ (mg/g)	5.131	7.468	6.293
	K_2 (g. mg^{-1} min^{-1})	0.018	0.018	0.019
	R^2	0.995	0.998	0.996
Intra-particle diffusion	$q_{e,exp}$ (mg/g)	2.417	4.371	3.532
	K_{id} (mg. g^{-1} $min^{-0.5}$)	0.206	0.236	0.211
	R^2	0.826	0.849	0.822

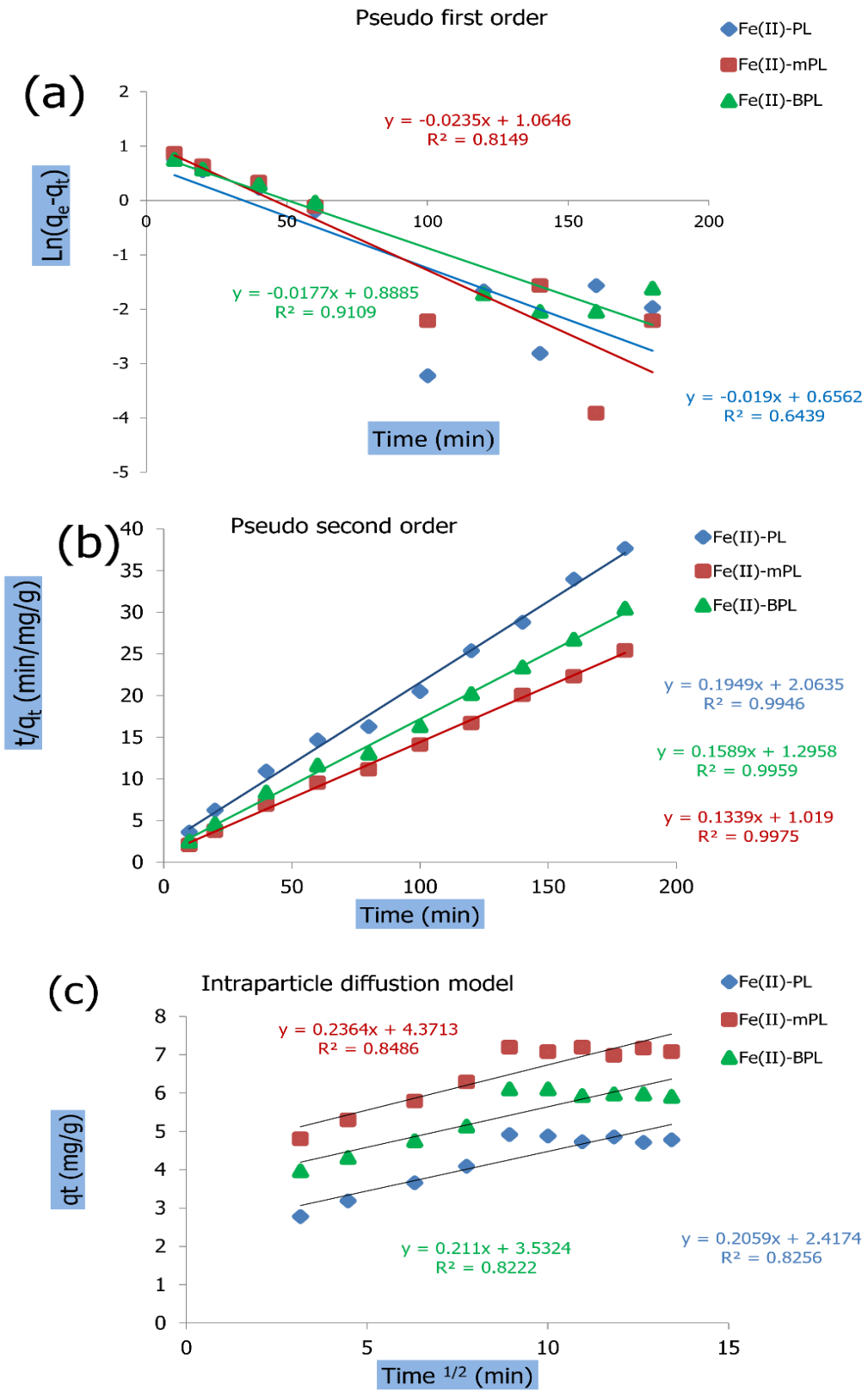

Figure 6 (a): Pseudo first order, (b) pseudo second order, and **(c)** intraparticle diffusion models.

4 Application of mPL for real samples

The elimination of Fe (II) ions by mPL for real samples from groundwater and a spiked Nile River sample is shown in the following **Table 4** with estimating TDS and pH.

Table 4: Application of Fe (II) ions removal by mPL for real samples.

Ground water									
Total dissolved salts (TDS) ppm		**pH**		**ICP method**			**Proposed method**		
Before adsorption	**After adsorption**	**Before adsorption**	**After adsorption**	**C_0**	**C_e**	**R %**	**C_0**	**C_e**	**R %**
863	845	5.040	6.430	1.672	0.128	92	1.614	0.161	90
A spiked Nile River sample									
Total dissolved salts (TDS) ppm		**pH**		**ICP method**			**Proposed method**		
Before adsorption	**After adsorption**	**Before adsorption**	**After adsorption**	**C_0**	**C_e**	**R %**	**C_0**	**C_e**	**R %**
214	193	5.070	6.820	5.103	0.267	95	5.071	0.286	94

5 Conclusions

Here, we prepared a low-cost adsorbent derived from palm leaves (PL) as adsorbent materials toward Fe (II) ions in the aqueous media. These materials are PL, modified PL (mPL) and biochar-derived from PL (BPL). The findings in our study showed that the surface area of both mPL and BPL are significantly larger than the pristine PL which is critical for the adsorbent process. The absorption of Fe (II) ions onto PL, mPL, and BPL fitted well with the Langmuir model. In addition, the kinetic analysis confirmed that the adsorption of Fe (II) ions onto our prepared adsorbents fitted with the pseudo-second-order model. Our work provides efficient and low-cost adsorbent materials for the elimination of Fe (II) ions from their aqueous solutions.

Acknowledgments: The authors would like to thank the head of chemistry department in faculty of science, Al-Azhar University.

Conflicts of interest: There are no conflicts to declare.

6 References

Abdelmonem, H. A., Hassanein, T. F., Sharafeldin, H. E., Gomaa, H., Ahmed, A. S. A., Abdel-lateef, A. M., Tilp, A. H. (2024). Cellulose-embedded polyacrylonitrile/amidoxime for the removal of cadmium (II) from wastewater: Adsorption performance and proposed mechanism. *Colloid. Surf. A: 684*, 133081. doi.org/10.1016/j.colsurfa.2023.133081

Abdelrazek, E. J. E., Gahlan, A. A., Gouda, G. A., Ahmed, A. S. A. (2025). Cost-effective adsorption of cationic dyes using ZnO nanorods supported by orange peel-derived carbon. *Sci. Rep., 15*(1), 4123. doi:10.1038/s41598-025-86209-2

Abu Al-Rub, F. A. (2006). Biosorption of zinc on palm tree leaves: equilibrium, kinetics, and thermodynamics studies .*Sep. Sci. Tech., 41*(15), 3499-3515. doi:10.1080/01496390600915015

Ali, A. F. M., Ahmed, A. S. A., Gahlan, A. A., El-sayed, A.-A. Y. (2024). Biochar derived from peanut husks as an adsorbent to ammonium ions remediation from aqueous solutions. *Egy. J. Chem., 67*(12), 231-244. doi:10.21608/ejchem.2024.271974.9374

Askari, R., Mohammadi, F., Moharrami, A., Afshin, S., Rashtbari, Y., Vosoughi, M., Dargahi, A. (2023). Synthesis of activated carbon from cherry tree waste and its application in

removing cationic red 14 dye from aqueous environments. *Appl. Water Sci., 13*(4), 90. doi:10.1007/s13201-023-01899-1

C, F. C., Kamalesh, T., Kumar, P. S., Rangasamy, G. (2023). A Critical review on the sustainable approaches for the removal of toxic heavy metals from water systems. *Indust. Eng. Chem. Res., 62*(22), 8575-8601. doi:10.1021/acs.iecr.3c00709

Cheira, M. F., Ahmed, A. S. A., Elshehy, E. A. (2024). 7 - Advances of 2D nanostructure-based membranes for water treatment and radioactive pollutants removal. In W. A. El-Said & N. Ghany (Eds.), *Functionalization of Two-Dimensional Materials and Their Applications* (pp. 209-270): Woodhead Publishing.

Denizli, A., Say, R., Arica, Y. (2000). Removal of heavy metal ions from aquatic solutions by membrane chromatography. *Sep. Purif. Tech., 21*(1), 181-190. doi.org/10.1016/S1383-5866(00)00203-3

Dey, S., Kotaru, N. S. A., Veerendra, G. T. N., Sambangi, A. (2022). The removal of iron from synthetic water by the applications of plants leaf biosorbents. *Clean. Eng. Tech., 9*, 100530. doi.org/10.1016/j.clet.2022.100530

Dutta, S., Gupta, B., Srivastava, S. K., Gupta, A. K. (2021). Recent advances on the removal of dyes from wastewater using various adsorbents: a critical review. *Mater. Adv., 2*(14), 4497-4531. doi:10.1039/D1MA00354B

El-Sawaf, A., A. Tolan, D., Abdelrahman, M. S., El-Hay, I. A., Ismael, M., Ahmed, A. S. A., Abdu, M. T .(2024) .Fast synthesis of mesoporous Prussian blue-silica nanocomposite for superior silver ions recovery performance. *J. Chem. Tech. Biotech., 99*(9), 1941-1954. doi.org/10.1002/jctb.7707

Ezeonuegbu, B. A., Machido, D. A., Whong, C. M. Z., Japhet, W. S., Alexiou, A., Elazab, S. T. Batiha, G. E. (2021). Agricultural waste of sugarcane bagasse as efficient adsorbent for lead and nickel removal from untreated wastewater: Biosorption, equilibrium isotherms, kinetics and desorption studies. *Biotechnol Rep, 30*, e00614. doi:10.1016/j.btre.2021.e00614

Guimarães, T., de Carvalho Teixeira, A. P., de Oliveira, A. F., Lopes, R. P. (2020). Biochars obtained from arabica coffee husks by a pyrolysis process: characterization and application in Fe(II) removal in aqueous systems. *N. J. Chem., 44*(8), 3310-3322. doi:10.1039/C9NJ04144C

Herbert, A., Kumar, U., Janardhan, P. (2021). Removal of hazardous dye from aqueous media using low-cost peanut (Arachis hypogaea) shells as adsorbents. *Water Environ. Res., 93*(7), 1032-1043. doi.org/10.1002/wer.1491

Khalid M. Khader, R. S. F., Moustafa M.S. Abo-Elfadl, Mohamed E.A. Ali (2022). Heavy metal ions and fluoride removal from wastewater using moringa seed beads. *Al-Azhar Bullet. Sci. 33*(1), 27-39 .

Krajčovičová, T. E., Hatala, M., Gemeiner, P., Híveš, J., Mackuľak, T., Nemčeková, K., Svitková, V. (2023). Biochar for water pollution control: from sensing to decontamination. *Chemosensors, 11*(7). doi:10.3390/chemosensors11070394

Li, L., Zhong, Y., Hu, Y., Bai, J., Qiao, F., Ahmed, A. S. A., Xie, Y. (2023). Room-temperature synthesis of Ag- and Mn-doped $Cs_2NaBiCl_6$ octahedrons for dye photodegradation. *CrystEngComm, 25*(30), 4355-4 .363doi:10.1039/D3CE00372H

Maneechakr, P., Karnjanakom, S. (2017). Adsorption behaviour of Fe(II) and Cr(VI) on activated carbon: Surface chemistry, isotherm, kinetic and thermodynamic studies. *J. Chem. Thermodyn., 106*, 104-112. doi.org/10.1016/j.jct.2016.11.021

Meez, E., Rahdar, A., Kyzas, G. Z. (2021). Sawdust for the removal of heavy metals from water: A review. *Molecules, 26*(14). doi:10.3390/molecules26144318

Moghadam, M. R., Nasirizadeh, N., Dashti, Z., Babanezhad, E. (2013). Removal of Fe(II) from aqueous solution using pomegranate peel carbon: equilibrium and kinetic studies. *Inter. J. Indust. Chem., 4*(1), 19. doi:10.1186/2228-5547-4-19

Mungondori, H. H., Mtetwa, S., Tichagwa, L., Katwire ,D. M., Nyamukamba, P. (2017). Synthesis and application of a ternary composite of clay, saw-dust and peanut husks in heavy metal adsorption. *Water Sci Technol, 75*(10), 2443-2453. doi:10.2166/wst.2017.123

Nilavazhagi, A., Felixkala, T. (2021). Adsorptive removal of Fe(II) ions from water using carbon derived from thermal/chemical treatment of agricultural waste biomass: Application in groundwater contamination. *Chemosphere, 282*, 131060. doi.org/10.1016/j.chemosphere.2021.131060

Ozcan, A., Oncü, E. M., Ozcan, A. S. (2006). Adsorption of Acid Blue 193 from aqueous solutions onto DEDMA-sepiolite. *J Hazard Mater, 129*(1-3), 244-252. doi:10.1016/j.jhazmat.2005.08.037

Popkin, B. M., D'Anci, K. E., Rosenberg, I. H. (2010). Water, hydration, and health. *Nutr Rev, 68*(8), 439-458. doi:10.1111/j.1753-4887.2010.00304.x

Qiu, C., Jiang, L., Gao, Y., Sheng, L. (2023). Effects of oxygen-containing functional groups on carbon materials in supercapacitors: A review. *Mater. Design, 230*, 111952 doi.org/10.1016/j.matdes.2023.111952

Ramos, C. G., Sousa, S. A., Grilo, A. M., Feliciano, J. R., Leitão, J. H. (2014). Retraction for Ramos et al., The second RNA chaperone, Hfq_2, is also required for survival under stress and full virulence of Burkholderia cenocepacia J2315. *J Bacteriol, 196*(22), 3980. doi:10.1128/jb.02242-14

Reda, F. A.-Z., El Refay, H., Goma, A., Badawy, N., Abufarha, S., El-Sayed, A. (2022). Bio-waste as eco-friendly adsorbent for the removal of hazardous dyes. *Al-Azhar Bullet. Sci., 33*(1), 1-13. doi.org/10.21608/absb.2022.105908.1152

Sarker, T. C., Azam, S. M. G. G., El-Gawad, A. M. A., Gaglione, S. A., Bonanomi, G. (2017). Sugarcane bagasse: a potential low-cost biosorbent for the removal of hazardous materials. *Clean Tech. Environ. Policy, 19*(10), 2343-2362. doi:10.1007/s10098-017-1429-7

Tamura, H., Goto, K., Yotsuyanagi, T., Nagayama, M. (1974). Spectrophotometric determination of iron(II) with 1,10-phenanthroline in the presence of large amounts of iron(III). *Talanta, 21*(4), 314-318. doi.org/10.1016/0039-9140(74)80012-3

Tolan, D., El-Sawaf, A., Ahmed, A. S. A., Nassar, A., Mohamed, N. M., Alhindawy, I. G., Utgikar, V. (2024). Enhanced photocatalytic activity of (In–Sr–P) tridoped TiO_2/Bi_2O_3 composite loaded on mesoporous carbon: A facile sol-hydrothermal synthesis approach. *Mater. Chem. Physi., 322*, 129570. .doi.org/10.1016/j.matchemphys.2024.129570

Türkmen, D., Bakhshpour, M., Akgönüllü, S., Aşır, S., Denizli, A. (2022). Heavy Metal Ions Removal From Wastewater Using Cryogels: A Review. *Front. Sustain., 3* .

Wang, S., Wang, N., Yao, K., Fan, Y., Li, W., Han, W., Chen, D. (2019). Characterization and interpretation of Cd (II) adsorption by different modified rice straws under contrasting conditions. *Sci. Rep., 9*(1), 17868. doi:10.1038/s41598-019-54337-1

Yefremova, S., Kablanbekov, A., Satbaev, B., Zharmenov, A. (2023). Rice Husk-based adsorbents for removal of metals from aqueous solutions. *Mater., 16*(23). doi:10.3390/ma16237353

Zhu, H. Y., Jiang, R., Xiao, L., Zeng, G. M. (2010). Preparation, characterization, adsorption kinetics and thermodynamics of novel magnetic chitosan enwrapping nanosized gamma-Fe_2O_3 and multi-walled carbon nanotubes with enhanced adsorption properties for methyl orange. *Bioresour Technol*, *101*(14), 5063-5069. doi:10.1016/j.biortech.2010.01.107